Structure and Properties of Cobalt-Exchanged H-ZSM5 Catalysts for Dehydrogenation and Dehydrocyclization of Alkanes

Wei Li,[‡] Sara Y. Yu,[‡] George D. Meitzner,[†] and Enrique Iglesia*[,‡]

Department of Chemical Engineering, University of California at Berkeley, Berkeley, California 94720, and Edge Analytical, 2126 Allen Blvd., Middleton, Wisconsin 53562

Received: June 12, 2000; In Final Form: November 14, 2000

Co/H-ZSM5 catalysts with Co/Al ratios of 0.09−0.22 were prepared by aqueous exchange. Turnover rates for propane conversion to propene and to C_6−C_8 aromatics on these catalysts are about 10-fold higher than on H-ZSM5. The selectivities to propene, aromatics, and H_2 are also higher on Co/H-ZSM5 than on H-ZSM5. The rate of D_2 exchange with OH groups increases with increasing Co/Al ratio, suggesting that Co cations catalyze D_2 dissociative chemisorption steps that limit the rate of isotopic exchange. Co cations also catalyze hydrogen recombinative desorption steps, which limit the rate of propane dehydrogenation and aromatization reactions. The density of residual zeolitic hydroxyls was measured by D_2−OH isotopic exchange and by changes in the intensity of OH infrared bands as a function of Co content. D_2−OH and infrared measurements showed that Co^{2+} cations replace 1.1−1.3 zeolitic protons, suggesting the predominant presence of Co^{2+}−O−Co^{2+} dimers, with some Co^{2+} monomers, each bridging two next-nearest neighbor Al sites. The location and structure of exchanged Co cations were probed using X-ray absorption spectroscopy (XAS) and temperature-programmed reduction (TPR). No H_2 consumption was detected up to 1273 K during TPR in any of the Co/H-ZSM5 samples, consistent with the absence of CoO_x crystallites, which reduce at ∼800 K. In situ near-edge X-ray absorption studies confirmed that Co species remain as divalent cations during exposure to H_2 or C_3H_8 at 773 K. Near-edge and fine structure analysis detected Co^{2+} cations with similar structure in all Co/H-ZSM5 samples (Co/Al < 0.22), and Co coordination changes from octahedral to tetrahedral upon sample dehydration at 773 K in He. Radial structure functions showed weak contributions from the first and second shells around Co. This reflects the nonuniform nature of the distance and orientation in Al−Al next-nearest neighbor sites in ZSM5.

Introduction

H-ZSM5 zeolites exchanged with Zn or Ga cations catalyze propane dehydrocyclodimerization via bifunctional pathways involving Brønsted acid sites and exchanged cations.[1−8] Cations increase propane conversion turnover rates and aromatics and H_2 formation rates by catalyzing the recombinative desorption of H_2, which occurs slowly on H-ZSM5.[8,9] Hydrogen desorption steps are not quasi-equilibrated during alkane reactions on cation-exchanged H-ZSM5. Catalytic sites provided by cations relieve the kinetic bottleneck that limits the rate and selectivity of alkane dehydrocyclodimerization reactions.

Here, we describe the structure and the catalytic properties of Co-exchanged H-ZSM5 materials; these materials have not been previously reported as alkane dehydrocyclodimerization catalysts. In this study, the density and structure of Co species and of Brønsted acid sites was measured by combining temperature-programmed reduction (TPR), D_2−OH isotopic exchange, infrared measurements, and X-ray absorption spectroscopy (XAS); their catalytic properties for propane dehydrocyclodimerization reactions were examined and compared with the behavior of H-ZSM5 and Zn/H-ZSM5.

Co/H-ZSM5 catalysts have been studied for the selective reduction of NO using alkanes.[10−12] Thus, these materials appear to contain catalytic sites for alkane activation reactions. Recently, we have shown that these materials also catalyze cross-hydrogenation reactions of alkane−thiophene mixtures with the selective formation of H_2S using adsorbed hydrogen formed in alkane C−H bond activation steps.[13,14] Co/H-ZSM5 materials have been previously prepared via aqueous [10,15] and solid-state exchange methods.[16] The resulting species have been characterized by temperature-programmed reduction (TPR),[15] X-ray diffraction (XRD), UV−visible,[15,17] electron paramagnetic resonance (EPR),[10] X-ray photoelectron (XPS),[10,15] and X-ray absorption (XAS) spectroscopies.[16] In these studies, the reported results were often limited to qualitative spectral information; also, the complementary information provided by these techniques was difficult to combine into a complete structural picture, because samples were prepared from different precursors and zeolitic materials in each study.

Here, we apply several complementary structural and chemical characterization methods to establish the structure and density of exchanged cations and of residual acidic OH groups in Co/H-ZSM5. The rate of reduction of Co^{2+} cations was used to detect CoO_x clusters and CoO or Co_3O_4 bulk crystallites. Infrared and isotopic exchange methods were used to measure the density of residual hydroxyls as the Co content was varied. Near-edge (XANES) and extended fine structure (EXAFS) X-ray absorption methods were used to determine the local coordination of Co^{2+} cations. These measurements led to a consistent model of Co^{2+} monomers and dimers bridging two neighboring cation-exchange sites provided by next-nearest

* Author to whom correspondence should be addressed. Fax: 510-642-4778. E-mail: iglesia@cchem.berkeley.edu.
[†] Edge Analytical.
[‡] University of California at Berkeley.

10.1021/jp002102h CCC: $20.00
Published on Web 01/19/2001

neighbor Al atoms in Co/H-ZSM5 (Co/Al = 0.09−0.22). These bridging Co cations catalyze dissociative adsorption of H_2 and the recombinative desorption of hydrogen adatoms and they lead to an increase in the rate of propane dehydrocyclodimerization reactions.

Experimental Section

Catalyst Synthesis. Co/H-ZSM5 samples were prepared by aqueous exchange of H-ZSM5 (prepared from Na-ZSM5; Zeochem, Si/Al = 14.5) with $Co(NO_3)_2$ ($Co(NO_3)_2 \cdot 6H_2O$, Aldrich, 99%) aqueous solutions at 353 K. The synthesis and characterization details of the H-ZSM5 sample are reported elsewhere.[7,18] The Co content in the exchanged samples was controlled by varying the exchange time of H-ZSM5 (~2.5 g each) with a 0.05 M $Co(NO_3)_2$ solution between 2 and 16 h, except for the sample with the highest cobalt loading (Co/Al = 0.22), which was prepared by exchanging H-ZSM5 with a 0.5 M $Co(NO_3)_2$ aqueous solution for 24 h at 353 K. After exchange, the samples were filtered, washed with deionized water (2 L), dried in ambient air overnight at 393 K, and treated in flowing dry air at 773 K (1.67 $cm^3\ s^{-1}$) for 20 h. The Co contents were measured by atomic absorption (Galbraith Laboratories, Inc.); they ranged from 0.46 to 1.1wt % Co, corresponding to Co/Al atomic ratios of 0.09−0.22. The higher Co contents reported in previous studies [12,15] were not achieved here, even though the $Co(NO_3)_2$ concentration of the exchange solution was higher in our synthesis procedures than in the previous studies.

Characterization Methods. Reduction rate measurements were carried out using a 19.1% H_2/Ar (Matheson, certified standard) stream by measuring the H_2 consumption rate using a modified Quantasorb apparatus (Quantachrome) equipped with a thermal conductivity detector. The system response was calibrated by reducing CuO (Fisher), CoO (Aldrich), and Co_3O_4 (Aldrich). The reducing gas mixture was metered using an electronic mass flow controller (Porter Instruments; 1.33 $cm^3\ s^{-1}$). Temperature-programmed reduction (TPR) measurements were carried out using 0.25 g of Co/H-ZSM5 by increasing the sample temperature from ambient to 1273 K at a rate of 0.167 $K\ s^{-1}$. Reduction rates are reported as the molar H_2 consumption rates per g-atom Co.

The density of zeolite OH groups remaining after ion exchange was obtained from the amount of HD and H_2 evolved during exchange of D_2 with OH groups, and also from the intensity of the infrared OH band in Co/H−ZSM5 samples. D_2−OH exchange experiments were carried out by raising the temperature of Co/H-ZSM5 or H-ZSM5 samples (0.2 g) to 773 K (973 K for H-ZSM5) at 0.167 $K\ s^{-1}$ in a flowing 5% D_2/Ar mixture (Matheson, certified standard, 1.67 $cm^3\ s^{-1}$) and measuring the concentrations of HD and H_2 in the effluent using mass spectrometry (Leybold-Inficon, Transpector Model). This technique measures the total number of OH groups. When silanol groups or extraframework Al are minority species, this method gives the density of acidic hydroxyls associated with framework Al. Infrared spectra were obtained using a Fourier transform infrared spectrometer (Mattson, Research Series), an in situ Praying-Mantis diffuse reflectance attachment (Harrick Scientific, DRP-XXX), and a flow cell (Harrick Scientific, HVC-DR2) equipped with NaCl windows. Infrared spectra are reported in pseudo-absorbance units, calculated from the reflected intensity using the Kubelka-Munk function [19] with KBr as the reference. Spectra were collected in the 400−4000 cm^{-1} frequency range with a resolution of 4 cm^{-1}.

X-ray absorption studies were performed at the Stanford Synchrotron Research Laboratory (SSRL) on beamlines 2-3 and 4-1 using an unfocused Si (111) double crystal upward-reflecting monochromator with parallel geometry. The intensities of the incident photon beam, the post-sample transmitted beam, and the transmitted beam after a reference Co foil were recorded using three N_2-purged ionization chambers. The energy was calibrated by concurrently measuring the sample spectrum and that for a Co foil (absorption edge energy of 7709 eV). X-ray absorption spectra were measured using an in-situ capillary cell and a portable gas manifold;[20] X-ray absorption data were analyzed using WinXAS (version 1.2).[21] A linear fit to the preedge region was subtracted from the entire spectrum, and then the spectrum was normalized using a fifth-order polynomial fit to the postedge (EXAFS) region. The energy scale for conversion to k (wave vector) space was calibrated by defining the first inflection point available in all the spectra, or the first inflection point beyond the preedge peak (if present), as the absorption edge. After conversion to k-space, the EXAFS weighted by k^1 was Fourier transformed between 2.5 and 15 $Å^{-1}$ using a Hanning's window function. Due to the weak EXAFS signals from Co in these samples, only one-shell fits to Co K-edge EXAFS were carried out for fresh and dehydrated samples. The single shell of oxygen neighbors was generated with FEFF 6.0.

Propane Reaction Rate and Selectivity on Co/H-ZSM5. The rate and the selectivity of propane reactions were measured in a recirculating batch reactor at 773 K.[8] The recirculation rate of the reactant flow was greater than 2 $cm^3\ s^{-1}$ in order to ensure low propane conversions per pass (<1%). Samples (~0.08 g) were treated in flowing air (1.67 $cm^3\ s^{-1}$) for 1 h at 773 K before propane reactions at 773 K and 110 kPa using a 20% C_3H_8/He (Praxair, certified mixture) recirculating reactant mixture. Reactant and product concentrations were measured as a function of contact time by injecting 0.2 cm^3 syringe gas samples into a gas chromatograph (Hewlett-Packard 5890) equipped with a capillary column (Hewlett-Packard, HP-1 methyl-silicone column, 50 m, 0.32-mm diameter, 1.05 μm film thickness) and a flame ionization detector. Batch reactor data are shown as turnovers (moles of propane converted per g-atom Al) or site-yields (moles of propane appearing as a given product per g-atom Al in samples) as a function of contact time. The slope of these plots gives the propane turnover rate or product site−time yield. Product selectivities are reported on a carbon basis, as the percentage of the converted propane appearing as a given product. H_2 selectivity is calculated from a hydrogen balance, as the percentage of the H atoms in the converted propane that do not appear within the observed hydrocarbon products.

Results and Discussion

Reduction of Co/H-ZSM5 in H_2. The reduction of Co/H-ZSM5 in H_2 was used to probe the reducibility of the Co species. H_2 consumption rates during reduction of CoO and Co_3O_4 and of Co/H-ZSM5 samples with Co/Al ratios of 0.09−0.22 are shown in Figure 1. CoO and Co_3O_4 powders reduced to Co metal below 800 K and the amount of H_2 consumed corresponded to H_2/Co ratios of 0.93 and 1.31, respectively; these values are very similar to those expected from stoichiometric complete reduction of CoO (1.0) and Co_3O_4 (1.33) to Co metal. In contrast, the amount of H_2 consumed during heating of Co/H-ZSM5 samples to 1273 K corresponded to H_2/Co ratios less than 0.01. Thus, Co species in these Co/H-ZSM5 samples remained essentially unreduced even at 1273 K for Co/Al ratios of 0.09−0.22. These data show that CoO_x clusters or crystallites are not present and that all Co^{2+} cations reside as dispersed species, presumably at cation exchange sites.

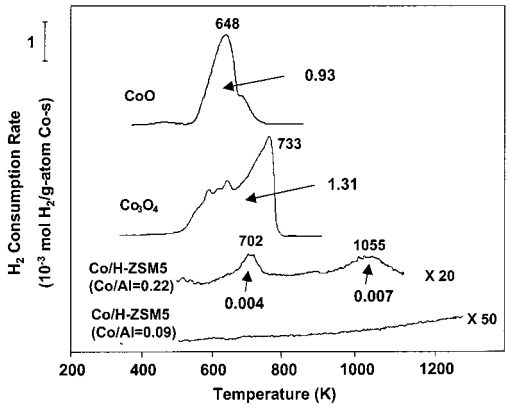

Figure 1. H_2 consumption rates during temperature-programmed reduction of CoO, Co_3O_4, and Co/H-ZSM5 (Co/Al = 0.09 and 0.22) [19.1% H_2/Ar, 1.33 cm^3 s^{-1}, 0.167 K s^{-1}]. The numbers next to the plot indicate the measured amount of H_2 consumed normalized to Co content, expressed as H_2/Co ratios.

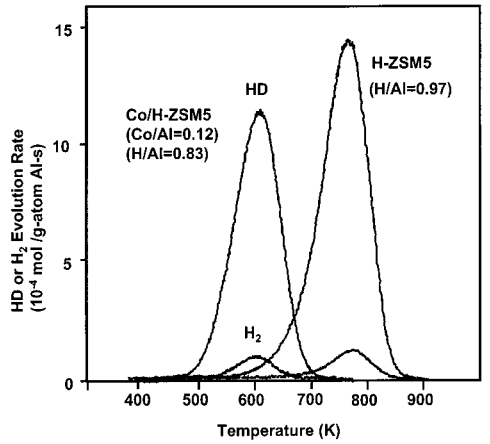

Figure 2. HD and H_2 formation rates during isotopic D_2−OH exchange experiments on H-ZSM5 and Co/H-ZSM5 (Co/Al = 0.12) [5% D_2/Ar, 1.67 cm^3 s^{-1}, 0.167 K s^{-1}].

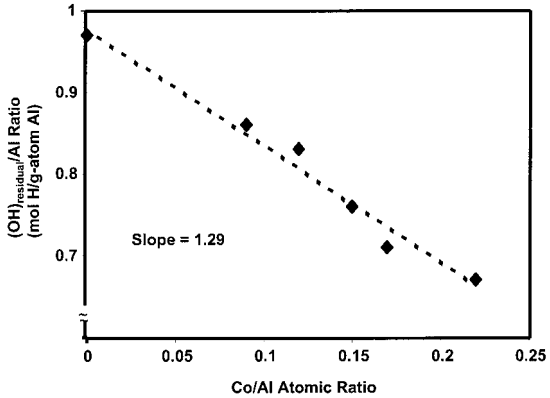

Figure 3. Density of residual hydroxyls as a function of Co/Al ratio from D_2−OH exchange experiments [5% D_2/Ar, 1.67 cm^3 s^{-1}, 0.167 K s^{-1}].

Exchanged Co^{2+} cations do not reduce in H_2 even at 1273 K, as also observed for exchanged Zn^{2+} in Zn/H-ZSM5.[7] The small but detectable H_2 consumption peaks at 702 and 1055 K for the sample with the highest Co loading (Co/Al = 0.22; H_2/Co < 0.01; Figure 1) may reflect the incipient formation of CoO_x clusters at high Co contents; these external CoO_x clusters appear to be responsible for the difficulties encountered in previous studies in establishing an accurate Co exchange stoichiometry.[16] The reduction peak at 702 K resembles that

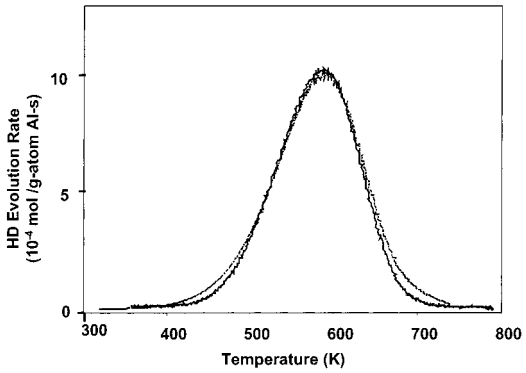

Figure 4. Comparison of the measured and calculated values of the HD evolution rate [Co/Al = 0.12, 5% D_2/Ar, 1.67 cm^3 s^{-1}, 0.167 K s^{-1}]. The thick solid line is the measured results, and the thin line is the calculated results.

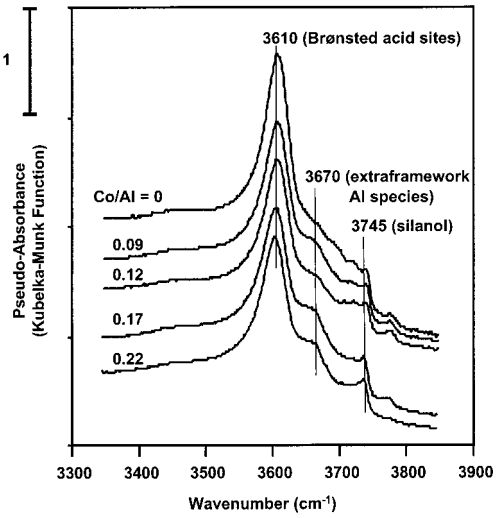

Figure 5. Infrared spectra of the OH stretching region for H-ZSM5 and Co/H-ZSM5 (Co/Al = 0.09−0.22).

observed at 733 K for the reduction of Co_3O_4, suggesting the incipient formation of bulk Co_3O_4. The H_2 consumption peak at 1055 K corresponds to traces of Co species that are less reducible than bulk cobalt oxides, possibly small CoO_x clusters interacting strongly with the external surface of ZSM5 crystals or Co silicates formed by interactions with silanol groups. The reduction process detected above 1000 K can also reflect changes in the coordination of exchanged Co^{2+} as the zeolite structure collapses, leading to the formation of reducible CoO_x crystallites. We conclude from these reduction measurements that more than 99% of the Co^{2+} cations in all of the Co/H-ZSM5 samples of this study exist in an environment that prevents their reduction. Such an environment is provided by cation exchange sites, which stabilize Co^{2+} against reduction, either by forming strong Co−O−Al bonds or by eliminating the possibility of the concerted agglomeration of Co^o required to nucleate stable Co metal clusters.

Previous temperature-programmed studies of Co/H-ZSM5 (Co/Al = 0.10−0.15) prepared by aqueous exchange [15] showed a H_2 consumption peak at ~1000 K, which was assigned to the reduction of Co^{2+} ions at cation exchange sites. No quantitative measure of the amount of H_2 consumed as a function of the Co content was reported. A similar H_2 consumption peak at 1055 K was observed in this study; we have assigned this peak to the reduction of CoO_x species. This peak cannot arise from the reduction of exchanged Co cations, because the amount of H_2 consumed would account for the reduction of less than 1% of

SCHEME 1: Steps of D_2-OH Exchange

$$D_2 + * \rightleftharpoons D_{mobile} + D^*$$

$$D_{mobile} + OH \rightleftharpoons H_{mobile} + OD$$

$$H_{mobile} + D^* \rightleftharpoons HD + *$$

the Co in these samples. The Co/H-ZSM5 samples in the previous study [15] may have included significant amounts of CoO_x clusters on external zeolite surfaces. These differences may reflect the high silanol concentration in the H-ZSM5 sample used in this study,[15] as evidenced by the reported infrared spectrum. These external silanol groups may allow strong interactions with hydrated Co species during aqueous exchange and lead to the formation of CoO_x clusters after treatment in air at high temperatures.

Density of Residual OH Groups after Exchange: Isotopic D_2-OH Exchange. HD and H_2 were formed as H atoms in the hydroxyl groups are replaced with D atoms when Co/H-ZSM5 samples are exposed to D_2 at temperatures above 450 K (Figure 2). HD was the predominant exchange product, but some H_2 was formed by secondary exchange of formed HD with the remaining OH groups. The presence of Co^{2+} species increased the rate of D_2-OH isotopic exchange and decreased the temperature of the HD evolution peak from 761 K on H-ZSM5 to 617 K on Co/H-ZSM5 (Co/Al = 0.12). On H-ZSM5, the (OH)/Al ratio was 0.97, suggesting the substantial absence of extraframework AlO_x species, a finding confirmed by ^{27}Al NMR measurements.[18] Also, infrared measurements indicated that there are few silanol groups on the external surface of the H-ZSM5 sample;[22] therefore, the predominant OH groups present in the H-ZSM5 sample and detected by the D_2-OH exchange process are acidic hydroxyls associated with framework Al cations. As a result, D_2-OH isotopic titrations accurately measure the number of exchange sites that retain a proton after exchange with Co^{2+} cations. The number of residual OH groups, $(OH)_{residual}$/Al ratio, is shown as a function of the atomic Co/Al ratio in Figure 3. The $(OH)_{residual}$/Al ratio decreased linearly with increasing Co/Al ratio; the slope of this linear response is ~1.3, suggesting that Co cations may exist as a mixture of several structures that replace between zero and two protons per Co atom. The linear dependence indicates that the exchange stoichiometry, and therefore the relative abundance of various exchanged cation structures, remains unchanged as the Co/Al ratio was varied (0.09−0.22).

D_2-OH exchange requires the dissociation of D_2 to form surface mobile D species, which then exchange with OH groups (Scheme 1). The exchange step of the mobile D species with the surface hydroxyls is quasi-equilibrated. Therefore, the measured HD evolution rates are given by the product of the D_2 dissociation rate and the probability that mobile D species find an unexchanged OH group among all surface hydroxyls ($x = [OH]_{remaining}/[OH]_{initial}$); this leads to first-order kinetics in OH surface density (Figure 4), as previously shown for Zn/H-ZSM5 samples.[7] As a result, the measured HD evolution rates reflect the rates of D_2 dissociation. The kinetic parameters corresponding to this first-order evolution peak were calculated by a regression fit of the measured rates in the range of $0.05 < x < 0.95$; the activation energies were 80 kJ mol^{-1} and 59 kJ mol^{-1} on H-ZSM5 and Co/H-ZSM5 (Co/Al = 0.12), respectively. A representative regression fit is shown in Figure 4. The activation energy on Co/H-ZSM5 samples did not change with Co/Al ratio (57−63 kJ mol^{-1}), suggesting that the rate depends on the intrinsic kinetics of D_2 dissociation on a distribution of Co^{2+} cation structures, which do not depend on the Co/Al ratio. The lower activation energy on Co/H-ZSM5 samples compared to the H−ZSM5 indicates that the addition of Co to H-ZSM5 substantially decreases the activation energy for the D_2 dissociation step, a necessary and rate-controlling step in the D_2-OH exchange reaction. As a result, Co species must also catalyze the microscopic reverse of the D_2 dissociation step, the recombinative desorption of hydrogens, a step that limits propane reactions on cation-exchanged H-ZSM5. Similar effects of Zn cations on D_2-OH exchange rates and activation energies were observed on Zn/H-ZSM5 catalysts.[7]

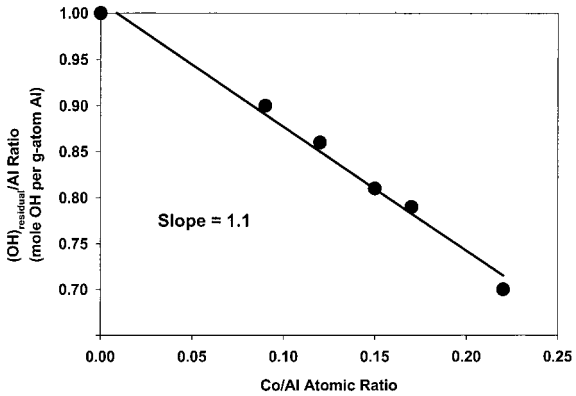

Figure 6. Density of residual hydroxyls obtained from infrared spectra for Co/H-ZSM5 with varying Co/Al ratio.

Density of Residual Hydroxyls from Infrared Measurements. Infrared spectra of Co/H-ZSM5 samples were measured in order to detect changes in the density of acidic hydroxyls after Co exchange. Three types of hydroxyl groups were detected by infrared in H-ZSM5: acidic hydroxyls associated with framework Al (Si−OH−Al), extraframework AlO_x-H species, and silanol (Si−OH) groups on external ZSM5 surfaces, with OH stretching bands at 3610, 3675, and 3745 cm^{-1}, respectively.[23,24] Figure 5 shows the OH stretching infrared region for Co/H-ZSM5 (Co/Al = 0.09−0.22) and H-ZSM5 samples. H-ZSM5 contains predominantly acidic OH groups with very few AlO_x-H or Si−OH groups; this is consistent with the OH/Al ratios near unity obtained from D_2-OH exchange measurements. The intensity of the OH band at 3610 cm^{-1} in Co/H-ZSM5 (Co/Al = 0−0.22), calibrated using the framework vibration bands at 500−1600 cm^{-1} as an internal standard, was normalized to the corresponding intensity in the unexchanged H-ZSM5 sample; this ratio was used to estimate the fraction of the acidic OH groups that remain after exchange, $[OH]_{residual}$/Al. This ratio decreased linearly with increasing Co/Al ratio with a slope of ~1.1 $(OH)_{removed}$ per Co (Figure 6). Thus, it appears that Co exchange can replace either zero, one, or two H^+ and that the exchange stoichiometry is essentially unaffected by the Co/Al ratio for values between 0.09 and 0.22. These conclusions are consistent with the D_2-OH exchange data shown in Figure 3. The intensities of the minority O−H bands for AlO_x-H and Si−OH species were not significantly affected by Co exchange, indicating that Co^{2+} cations do not interact with such species during exchange. It was reported previously[16] that the removal of acid sites, detected by infrared measurements of OH bands, was complete only for Co/Al ratios greater than one, leading these authors to conclude that exchange occurred with the replacement of one H^+ with each Co^{2+}. No evidence, however, was reported that all the Co atoms actually resided at cation exchange sites. The presence of CoO_x clusters

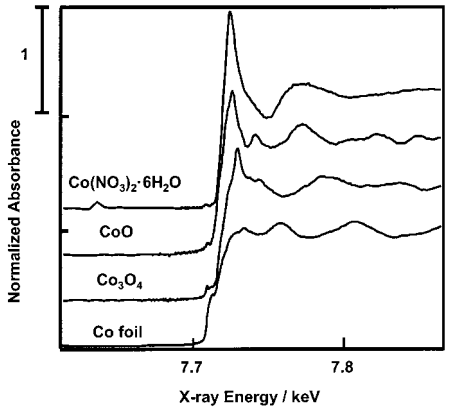

Figure 7. Near-edge spectra of Co metal, CoO, Co_3O_4, and $Co(NO_3)_2 \cdot 6H_2O$ standards at ambient conditions.

TABLE 1: Co K-Edge Energy Position for Co/H-ZSM5 Samples with Respect to That for Co Metal Foil (7.7090 keV)[a]

compound	edge position ΔE (eV)
Co foil	0
CoO	11.9
Co_3O_4	12.9
$Co(NO_3) \cdot 6H_2O$	13.5
Co/H-ZSM5 (Co/Al = 0.09)	13.1
Co/H-ZSM5 (Co/Al = 0.12)	13.2
Co/H-ZSM5 (Co/Al = 0.17)	13.1
Co/H-ZSM5 (Co/Al = 0.22)	13.2

[a] The edge position is defined as the first inflection point.

or bulk crystallites can lead to apparent Co content requirements larger than the stoichiometric amount needed for the complete titration of exchange sites.

Near-Edge and Extended Fine Structure X-ray Absorption Spectra (XAS). Figure 7 shows the near-edge X-ray absorption spectra (XANES) for Co metal, CoO, Co_3O_4, and $Co(NO_3)_2 \cdot 6H_2O$ standard materials at ambient conditions. Co_3O_4 shows a pre-edge peak, corresponding to 1s to 3d transitions that are forbidden in the centrosymmetric octahedral structures present in Co and CoO.[25] Distortion of this octahedral symmetry allows this transition to occur in Co_3O_4, which has 2/3 of its Co atoms in octahedral sites and the rest in tetrahedral sites.[26] As a result, a pre-edge feature is clearly detected in Co_3O_4 (Figure 7). The position of the absorption edge, defined as the first inflection point in the absorption edge for each sample reflects the Co oxidation state.[27] The absorption edge shifts to lower energy as Co^{2+} is reduced to Co metal.[25] Co K-edge energies are reported for all the Co/H-ZSM5 and for the reference Co compounds in Table 1. The absorption edge in Co/H-ZSM5 samples is ~13 eV higher than for Co foil and it is similar to that in $Co(NO_3)_2 \cdot 6H_2O$, consistent with the predominant presence of Co^{2+} cations in all Co/H-ZSM5 samples.

The near-edge spectra of all fresh (air-exposed) Co/H-ZSM5 samples (Co/Al = 0.09−0.22) are very similar (Figure 8), suggesting that Co^{2+} species reside at similar locations in all samples. The near-edge spectra of all air-exposed Co/H-ZSM5 samples resemble that of the $Co(NO_3)_2 \cdot 6H_2O$ standard (Figure 8), suggesting that hydrated Co^{2+} cations acquire octahedral coordination by adsorbing water molecules. CoO or Co_3O_4 standards show intense features corresponding to multiple coordination shells in the radial structure function (Figure 9). In contrast, the radial structure function for Co/H-ZSM5 samples shows few structural features beyond the first oxygen coordination shell (Figure 10), suggesting the substantial absence of

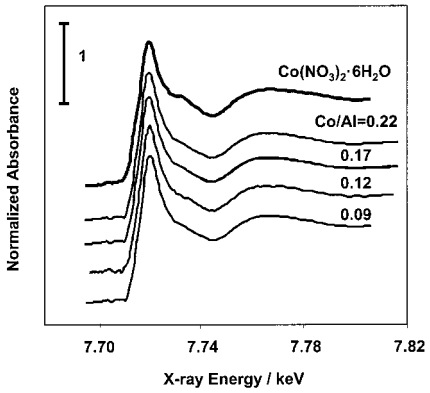

Figure 8. Near-edge spectra of fresh (hydrated) Co/H-ZSM5 samples (Co/Al = 0.09−0.22). The near-edge spectrum of $Co(NO_3)_2 \cdot 6H_2O$ standard is also shown for comparison.

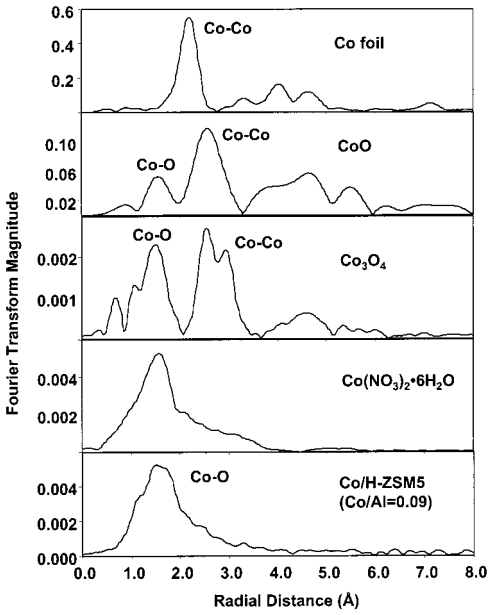

Figure 9. Radial structure functions of Co species in Co metal, CoO, Co_3O_4, and $Co(NO_3)_2 \cdot 6H_2O$ standards.

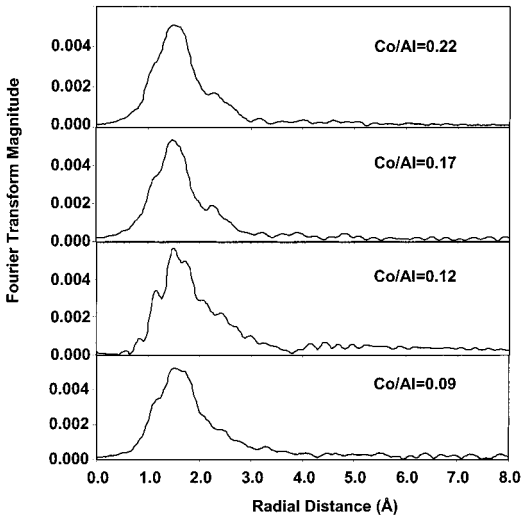

Figure 10. Radial structure functions of fresh (hydrated) Co/H-ZSM5 samples (Co/Al = 0.09−0.22) at ambient conditions.

longer-range coordination shells. Thus, Co^{2+} cations appear to reside at cation exchange sites as dispersed species and the location of the framework Al and Si atoms in more distant

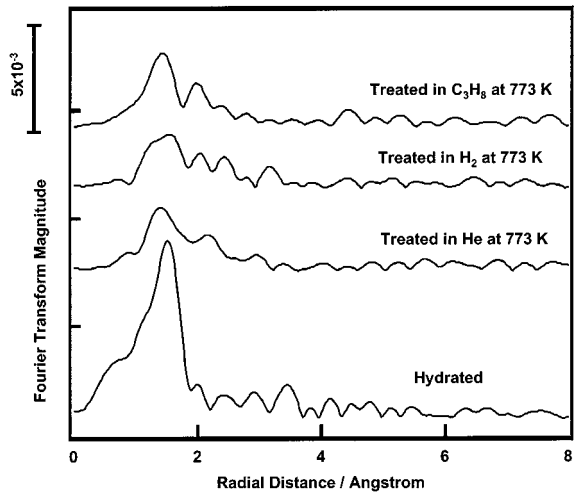

Figure 11. Radial structure functions of Co species in Co/H-ZSM5 (Co/Al = 0.22) in varying conditions: fresh(hydrated), in He at 773 K, in H_2 at 773 K, and in C_3H_8 at 773 K.

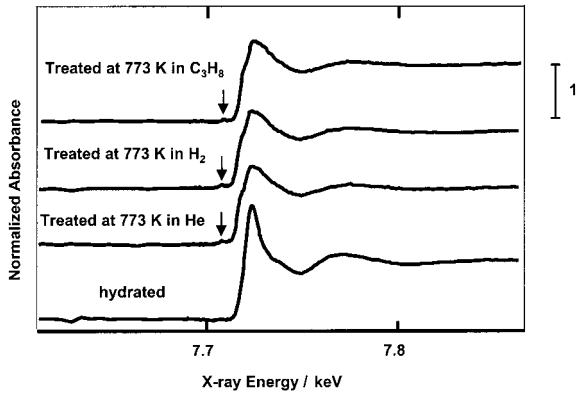

Figure 12. Near-edge spectra for Co/H-ZSM5 (Co/Al = 0.22): fresh-(hydrated) (a), in He at 773 K(b), in H_2 at 773 K(c), and in C_3H_8 at 773 K(d).

coordination spheres is highly nonuniform. As a result, neighbors beyond the bonded oxygen atoms do not contribute significantly to the radial structure function of Co/H-ZSM5 samples. The radial structure functions of fresh (air-exposed) Co/H-ZSM5 samples resemble that of $Co(NO_3)_2 \cdot 6H_2O$, with a broad Co−O shell at ~1.7 Å, indicating that Co^{2+} cations reside in an octahedral structure with the Co−O first coordination shell satisfied by framework O-atoms and by oxygen atoms in adsorbed H_2O (Figure 9). The radial structure functions in Co/H-ZSM5 samples with varying Co content are similar, indicating that they contain Co species with similar structure (Figure 10).

After dehydration in He at 773 K, the first coordination shell in the radial structure function of Co/H-ZSM5 (Co/Al = 0.22) became weaker, suggesting that the removal of water changes the local environment around Co^{2+} (Figure 11). Concurrently, a weak preedge feature appeared in the near-edge spectrum (Figure 12), indicating that the local symmetry of Co coordination changes from octahedral in hydrated samples to a less symmetric structure as coordinated water molecules are removed. The resulting distortion from the centrosymmetric octahedral structure allows 1s → 3d transitions to occur (Figure 12). This reversible effect of adsorbed water also provides indirect evidence for the dispersed nature of Co^{2+} species, which allows most of the Co^{2+} centers to be accessible at surfaces and to interact with water.

Treatments in H_2 or C_3H_8 up to 773 K did not change the near-edge spectrum (Figure 12), suggesting that the local Co coordination is unchanged by propane reactions or by H_2 treatment. Treatments in He, H_2, or C_3H_8 at 773 K also did not lead to a detectable shift in the absorption edge energy (Table 2), indicating that Co remained as divalent cations, in agreement with the TPR results, which showed that Co^{2+} species in Co/H-ZSM5 do not reduce in H_2 even at 1273 K.

TABLE 2: Co K-Edge Energy Position with Respect to That for Co Metal Foil (7709 eV) for Co/H-ZSM5 (Co/Al = 0.22) after Treatments at 773 K in He, H_2, or C_3H_8[a]

conditions	edge energy ΔE (eV)
ambient	13.2
He, 773 K	13.0
H_2, 773 K	13.1
C_3H_8, 773 K	13.0

[a] The edge position is defined as the first inflection point available in all spectra.

The radial structure functions of the Co species in Co/H-ZSM5 (Co/Al = 0.22) after treatment at 773 K in He, H_2, or C_3H_8 show weak features (Figure 11), suggesting that Co species reside in a non-uniform environment. Co^{2+} species assume a range of structures apparently as the result of the varying distances between framework oxygen atoms in the Al−Al next-nearest neighbor pairs required to coordinate Co^{2+} cations. This range of possible structures is consistent with the proposed bridging structures of the Co monomers and dimers (Scheme 2), which require interactions with Al−Al next-nearest neighbor sites and their associated framework oxygens. These oxygen atoms can assume a wide range of geometries, depending on the location of the Al−Al pairs within the zeolite channel. This leads to static disorder around Co^{2+} cations and to diffuse scattering features in the radial structure functions. Similar radial structure functions were previously reported on Co/H-ZSM5 samples prepared by $CoCl_2$ solid-state exchange,[16] for which only chlorine neighbors in the first Co coordination shell were observed. These authors concluded that a wide range of Co−O bond distances led to static distortion and prevented the detection of O nearest neighbors in the radial structure function.

One-shell fits to Co K-edge EXAFS from the fresh and dehydrated Co/H-ZSM5 samples were carried out using a single shell of oxygen neighbors generated with FEFF. EXAFS fits indicate octahedrally coordinated Co, with single Co−O distance of 2.086−2.096 Å, in all fresh samples (Co/Al = 0.09−0.22) (Table 3). Following dehydration at 773 K in He, Co in Co/H-ZSM5 (Co/Al = 0.09) has tetrahedral coordination by oxygen at single Co−O distance of 1.989 Å (Table 3). This is in agreement with our earlier finding based on analysis of the Co K-edge near-edge features that Co coordination in Co/H-ZSM5 samples changes from octahedral to tetrahedral upon dehydration.

Propane Dehydrocyclodimerization on Co/H-ZSM5, H-ZSM5, and Zn/H-ZSM5. Reaction rates and product selectivities (at ~11% propane conversion) on Co/H-ZSM5 are compared to those on H-ZSM5 and Zn/H-ZSM5 (with similar M/Al ratio) in Table 4. The exchange of protons in H-ZSM5 with Co^{2+} cations significantly increased initial propane conversion turnover rates (per Al), from 9.6×10^{-4} s^{-1} on H-ZSM5 to 2.6×10^{-3} s^{-1} on Co-ZSM5 (Co/Al = 0.12) and to 4.2×10^{-3} s^{-1} on Co-ZSM5 (Co/Al = 0.22). Initial propane conversion turnover rates reflect the rates of propane cracking and propane dehydrogenation, both of which increased with increasing Co content (Table 4). Also, aromatics site-time yields (per Al) increased from 0.41×10^{-4} s^{-1} on H-ZSM5 to 2.9×10^{-4} s^{-1} on Co/H-ZSM5 (Co/Al = 0.12). The selectivity to dehydrogenated products (propene and C_6−C_8 aromatics) increased, and

SCHEME 2: Formation of Exchanged Hydrated Co^{2+} Cations

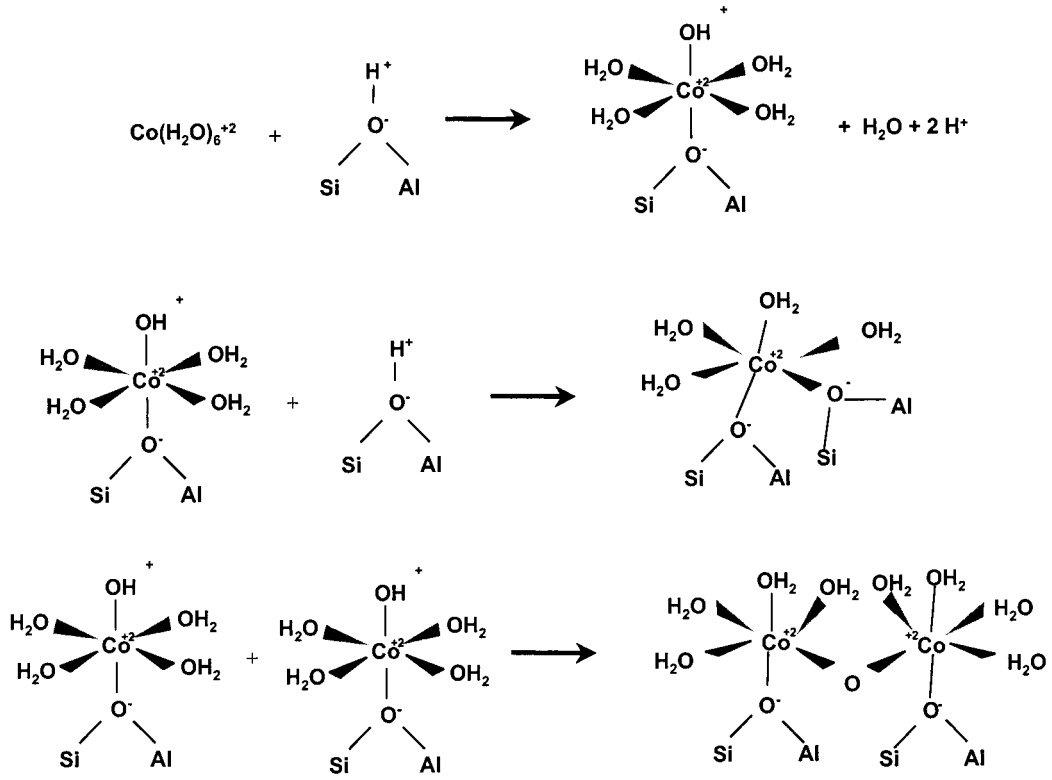

TABLE 3: One-Shell Fits to Co K-Edge EXAFS from Fresh and Dehydrated Co/H-ZSM5 Samples (Co/Al = 0.09−0.22) Using a Single Shell of Oxygen Neighbors Generated with FEFF[a]

sample	coord. no.	distance/Å	σ^2/Å^2	E_0 shift/eV
fresh, Co/Al = 0.09	6.0	2.079	0.004	−1.5
fresh, Co/Al = 0.12	6.4	2.090	0.011	−1.0
fresh, Co/Al = 0.17	5.9	2.076	0.008	−1.5
fresh, Co/Al = 0.22	6.5	2.096	0.011	−1.2
dehydrated, Co/Al = 0.09	4.3	1.991	0.011	0.5

[a] Co−O coordination number decreases from about 6 to 4 upon sample dehydration, indicating a Co coordination change from octahedral to tetrahedral. σ^2 is the Debye−Waller factor.

TABLE 4: Propane Turnover Rates and Product Distribution on H-ZSM5, 1.1% Co/H-ZSM5, and 1.3% Zn/H-ZSM5 [773 K, 21.5 kPa C_3H_8, Balance He]

	H-ZSM5	Co/H-ZSM5	Zn/H-ZSM5
M (wt %)	0.0	Co (1.1)	Zn (1.3)
M/Al	0.00	0.22	0.20
initial propane turnover rate (per Al, 10^{-3} s^{-1})	0.96	4.2	6.8
initial cracking rate (per Al, 10^{-3} s^{-1})	0.60	0.85	1.6
initial propene formation rate (per Al, 10^{-3} s^{-1})	0.36	3.0	4.5
propane conversion (%)	11.4	11.2	11.2
aromatics formation rate (per Al, 10^{-3} s^{-1})	0.041	0.56	2.0
carbon selectivity (%)			
methane	18.4	7.2	7.2
ethene	31.5	17.0	14.7
ethane	6.7	5.6	3.4
propene	24.7	41.6	33.8
C_6−C_8 aromatics	4.4	18.8	37.4
hydrogen selectivity (%)	9.1	23.5	31.3

the selectivity to the hydrogen-rich lighter products (methane and ethane) decreased, with increasing Co content. These effects

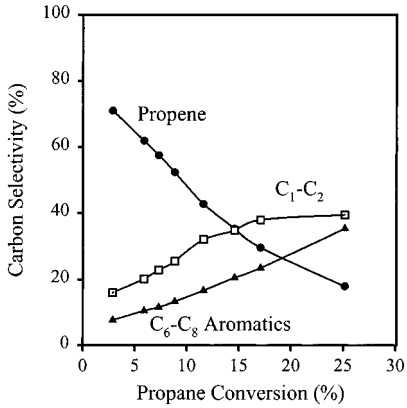

Figure 13. Product selectivities as a function of propane conversion on Co/H-ZSM5 [Co/Al = 0.17, 773 K, 21.5 kPa C_3H_8, balance He].

reflect the ability of Co^{2+} sites to desorb H atoms formed in C−H bond activation steps as H_2, as shown previously for Zn cations.[1,6−8]

The effects of contact time on conversion and selectivity are similar on Co/H-ZSM5 samples with a wide range of Co/Al ratios; these trends are shown in Figure 13 for the sample with a Co/Al of 0.17. The selectivities to C_1−C_2 and propene products show a non-zero intercept suggesting that these products can form via primary cracking reactions of propane. Ethane and C_6−C_8 aromatics are secondary products; they show very low initial selectivities, which increase with increasing contact time. The observed decrease in the selectivity to propene with increasing contact time (Figure 13) is caused by its secondary conversion to aromatics. Aromatics form predominately via acid-catalyzed, cation-assisted secondary reactions involving oligomerization, dehydrogenation, and cracking of alkenes, as previously shown on Zn- and Ga-exchanged H-ZSM5 catalysts.[3,6−8]

Initial propane conversion turnover rates and aromatics site-time yields increased with increasing Co content (Figure 14),

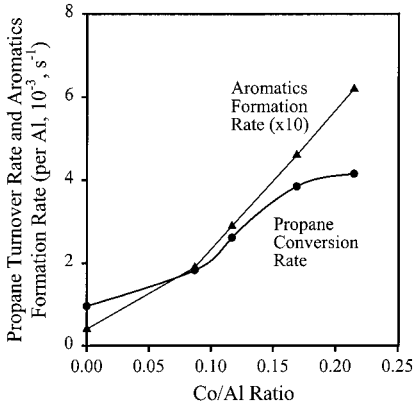

Figure 14. Initial propane turnover rate and aromatics site-time yield (at 10% propane conversion) as a function of Co/Al ratio [773 K, 21.5 kPa C_3H_8, balance He].

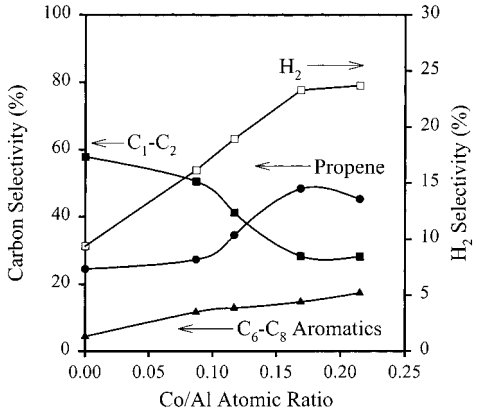

Figure 15. Product selectivities at 10% conversion as a function of Co/Al ratio [773 K, 21.5 kPa C_3H_8, balance He].

indicating that the rate-limiting step for propane dehydrogenation is catalyzed by Co cations. The effects of Co on the product selectivity are shown in Figure 15 at the same propane conversion (~10%). C_1-C_2 selectivity decreased and C_6-C_8 aromatics selectivity increased with increasing Co content, indicating that the addition of Co favors the formation of dehydrogenated products. Propene selectivities initially increased with increasing Co content, but then reached a constant value, apparently as the result of the ability of Co cations to increase also the rates of propene conversion to aromatics. H_2 selectivities increased with increasing Co content (Figure 15), suggesting that Co^{2+} cations increase the rate of recombinative desorption of hydrogen to form H_2. The rate-determining nature of hydrogen removal steps and the role of Zn cations as recombinative desorption sites were first proposed by Mole et al.[1] The similar role of Ga and Zn cations, as sites for the recombinative desorption of H_2, was later confirmed by kinetic and isotopic tracer studies.[6,9] The higher propane conversion and aromatics formation rates and the higher selectivities to dehydrogenated products and to H_2 observed as the Co content increases suggest a similar role of Co^{2+} cations in propane reaction pathways.

Initial propane dehydrogenation turnover rates (per Al) (total propane turnover rate minus cracking rate) on Zn/H-ZSM5 (Zn/Al = 0.20; 5.2×10^{-3} s^{-1}) are higher than on Co/H-ZSM5 (Co/Al = 0.22; 3.3×10^{-3} s^{-1}) (Table 4). Also, a higher selectivity to propene and a lower selectivity to C_6-C_8 aromatics are observed on Co/H-ZSM5 than on Zn/H-ZSM5. These results suggest that Zn^{2+} cations are more effective than Co^{2+} cations at catalyzing H_2 recombinative desorption. This is consistent

SCHEME 3: Consecutive Steps in Propane Dehydrogenation Reactions

$$C_3H_8 \xrightarrow[-H_2]{k_1} C_3H_6 \xrightarrow[-1.5\ H_2]{k_2} \frac{1}{2}C_6H_6$$

with the D_2-OH exchange results which showed the rates of D_2-OH isotopic exchange are faster on Zn/H-ZSM5 than on Co/H-ZSM5 and the temperature of the HD evolution peak is lower on Zn/H-ZSM5 (584 K, Zn/Al = 0.10) than on Co/H-ZSM5 (617 K, Co/Al = 0.12). This indicates that Zn cations are more effective in recombining surface hydrogens formed in C−H bond activation steps, leading to the more effective relief of kinetic bottlenecks and to higher propane turnover rates. As mentioned earlier, the primary product of propane dehydrogenation is propene, which undergoes secondary reactions to form aromatics, thus the reaction pathways can be considered as simple two-step consecutive reactions (Scheme 3), with k_1 and k_2 as the rate constants of each step. In the first step, each propane needs to lose only two hydrogens to form propene; in contrast, two propene molecules will have to each lose three hydrogens to form benzene, a representative aromatic product. As a result, k_2 is more sensitive than k_1 to the hydrogen removal capability of the cations. Since Co is not as effective as Zn in removing hydrogens, k_2 reflects these effects more sensitively than k_1; therefore, higher propene and lower aromatics selectivities are obtained on Co than on Zn when compared at similar propane conversion (~11%).

Structure and Density of Co Cations and Brønsted Acid Sites. Infrared and D_2-OH exchange measurements (Figures 3 and 6) show that each Co atom replaces about 1.1−1.3 protons during exchange. This stoichiometry suggests that some Co^{2+} cations replace two protons while others replace either one proton or none. A $H_{removed}$/Co value of two and charge neutrality requirements for Co^{2+} cations would require a bridging monomer interacting with two Al sites (Scheme 2). Such species may form via condensation of the initially exchanged $(Co-OH)(H_2O)_n^+$ with OH^+ (Scheme 2b). Isolated $(Co-OH)^+$ species, unable to condense, would not lead to the net removal of H atoms during exchange. $(Co-O-Co)^{2+}$ bridging dimers formed via condensation of two $(Co-OH)^+$ and interacting with two next-nearest neighbor Al sites would lead to the removal of only one H per exchanged Co^{2+} (Scheme 2c). The observed $OH_{removed}$/Co ratio of 1.1−1.3 (from D_2-OH and infrared measurements) would suggest that it is likely that Co cations can exist as bridging $(Co-O-Co)^{2+}$ dimers, Co^{2+} monomers, and isolated $(Co-OH)^+$. Reduction kinetic measurements showed that less than 1% of the Co atoms in these Co/H-ZSM5 samples can be reduced at temperatures below 1273 K, indicating the essential absence of CoO_x clusters or crystallites. The unreducible nature of Co species suggests that they exist predominantly as Co^{2+} monomers and $(Co-O-Co)^{2+}$ dimers. $(Co-OH)^+$ are expected to be more reducible than bridging Co monomers or dimers, by analogy with the properties for similar $(Zn-OH)^+$ species detected in Zn-exchanged Na-ZSM5 samples.[28]

Both the bridging Co^{2+} monomers and $(Co-O-Co)^{2+}$ dimers shown in Scheme 2 require the presence of next-nearest neighbor (NNN) Al−Al pairs within a certain distance. As a result, the maximum extent of Co exchange depends on the concentration of such Al pairs. A previous study of the Al location in ZSM5 [29] showed that a large fraction of Al atoms have Al next-nearest neighbors, residing within 4.2−6.5 Å of each other for Si/Al ratios of 11 to 19. A more recent study,[30] which excludes NNN pairs on opposite sides of a channel wall, concludes that M^{2+}/

Al ratios of ~0.15 are possible for the Si/Al ratio of 14.5 in our samples, if we assume that Co^{2+} cations exist exclusively as bridging monomers that span a distance of up to 5.5 Å between framework oxygen atoms. The presence of $(Co-O-Co)^{2+}$ dimers would increase the number of NNN Al−Al pairs because of the larger distance between Al pairs in these structures, consistent with the presence of isolated Co^{2+} monomers and dimers in samples with Co/Al ratios as high as 0.22.

Three types of exchanged Co^{2+} ions located at different cationic sites in Co/H-ZSM5 were suggested on the basis of a study using diffuse reflectance spectroscopy,[31] and the predominant Co species reside at distorted six-member rings at the intersection of straight and sinusoidal channels. However, only monomeric Co species were considered in this study, while our results cast significant doubts about the significant abundance of such monomers. Our deuterium titration measurements of the residual proton density in H-ZSM5 after Co exchange showed the predominant presence of $(Co-O-Co)^{2+}$ dimers in all samples. Our XAS measurements also suggest that Co exists as a mixture of Co-oxo species with varying Co−O bond distances and angles. The specific siting of each Co species, however, cannot be accurately determined due to the nonuniform nature of the distance and orientation in Al−Al next-nearest neighbors in ZSM5.

Structural and Functional Requirements in Alkane Reactions Catalyzed by Cation-Exchanged H-ZSM5. The exchange of protons by Co increases propane conversion rates and the rates of formation of desired dehydrogenated products (propene and aromatics). Co/H-ZSM5 shows similar qualitative behavior to Zn/H-ZSM5 and Ga/H-ZSM5. The role of Co cations in desorbing the H atoms formed in C−H bond activation steps as H_2 is consistent with D_2-OH measurements, which showed a substantial decrease in the activation energy for D_2-dissociation when Co was exchanged onto H-ZSM5. Co cations decrease the concentration of surface hydrogen atoms during propane reactions and the hydrogen content in the products of this reaction. As a result, propene and aromatics selectivities increase and C_1-C_2 selectivities decrease with increasing Co content (Figure 15).

The anchoring of Co^{2+} cations at exchange sites places them in close proximity to acid sites, which may be required for the effective transfer of hydrogens, formed at acid sites during alkane dehydrogenation or olefin dehydrocyclization steps, to cations for removal as H_2. The exchanged cations are isolated and coordinated strongly to the framework oxygen atoms. This appears to prevent their reduction and their ultimate agglomeration into Co^0 clusters, which would otherwise occur for CoO_x crystallites during propane reactions at high temperatures. The formation of metal clusters, if they remained well-dispersed, would effectively catalyze the desorption of hydrogen, but to such an extent that it may lead to the extensive dehydrogenation of adsorbed intermediates and to the rapid formation of deactivating deposits.

Conclusions

Propane dehydrogenation rates on cobalt-exchanged H-ZSM5 catalysts (Co/Al = 0.09−0.22) are about 10-fold higher than on H-ZSM5. The selectivities to propene, aromatics, and H_2 are also higher as Co is exchanged onto H-ZSM5. D_2-OH and infrared measurements showed that each Co^{2+} cation replaces about 1.1−1.3 zeolitic H^+, suggesting the presence of monomer and dimer Co species bridging two next-nearest neighbor Al sites. No significant H_2 consumption was detected up to 1273 K in any of the Co/H-ZSM5 samples, consistent with the absence of CoO_x crystallites, which reduce below 1000 K. In situ near-edge X-ray absorption (XAS) studies indicate that Co species exist at cation exchange sites with tetrahedral coordination after dehydration and that they remain as divalent cations during exposure to H_2 or to C_3H_8 at 773 K. Near-edge and fine structure analysis of XAS data showed the presence of well-dispersed Co^{2+} cations in all Co/H-ZSM5 samples (Co/Al < 0.22), indicating the formation of similar exchanged species at all Co contents. The radial structure functions showed weak contributions from the coordination shells (beyond the initial Co−O shell) around Co cations, a finding that we attribute to the nonuniform distributions of distances and orientations in Al−Al next-nearest neighbors in ZSM5 structures.

Acknowledgment. This work was supported by the National Science Foundation (CTS-96-13632). X-ray absorption data were collected at Stanford Synchrotron Radiation Laboratory (SSRL), a facility operated by the United States Department of Energy (DOE), Office of Basic Energy Sciences, under contract DE-ACO03-76SF00515. The authors acknowledge Ms. Grace J. Yu for the experimental assistance in obtaining the results shown in Figures 13−15.

References and Notes

(1) Mole, T.; Anderson, J. R.; Creer, G. *Appl. Catal.* **1985**, *17*, 141.
(2) Kitagawa, H.; Sendodo, Y.; Ono, Y. *J. Catal.* **1986**, *101*, 12.
(3) Gnep, N. S.; Doyemet, J. Y.; Guisnet, M. *J. Mol. Catal.* **1988**, *45*, 281.
(4) Iglesia, E.; Baumgartner, J. E.; Price, G. L. *J. Catal.* **1992**, *134*, 549.
(5) Ono, Y. *Catal. Rev.−Sci. Eng.* **1992**, *34*, 179.
(6) Biscardi, J. A.; Iglesia, E. *Catal. Today* **1996**, *31*, 207.
(7) Biscardi, J. A.; Meitzner, G. D.; Iglesia, E. *J. Catal.* **1998**, *179*, 192.
(8) Biscardi, J. A.; Iglesia, E. *J. Catal.* **1999**, *182*, 117.
(9) Biscardi, J. A.; Iglesia, E. *J. Phys. Chem. B* **1998**, *102*, 9284.
(10) Sun, T.; Trudeau, M. L.; Ying, J. Y. *J. Phys. Chem.* **1996**, *100*, 13662.
(11) Okada, O.; Tabata, T.; Kokitsu, M.; Ohtsuka, H.; Sabatino, L. M. F.; Belluussi, G. *Appl. Surf. Sci.* **1997**, *121/122*, 267.
(12) Desai, A. J.; Kovalchuk, V. I.; Lombardo, E.; d'Itri, J. L. *J. Catal.* **1999**, *184*, 396.
(13) Yu, S. Y.; Li, W.; Iglesia, E. *J. Catal.* **1999**, *187*, 257.
(14) Li, W.; Yu, S. Y.; Iglesia, E. *Stud. Surf. Sci. Catal.* **2000**, *130*, 899.
(15) da Cruz, R. S.; Mascarenhas, A. J. S.; Andrade, H. M. C. *Appl. Catal. B* **1998**, *18*, 223.
(16) Jentys, A.; Lugstein, A.; Vinek, H. *J. Chem. Soc., Faraday Trans.* **1997**, *93*, 4091.
(17) Verberckmoes, A. A.; Weckhuysen, B. M.; Pelgrims, J.; Schoonheydt, R. A. *J. Phys. Chem.* **1995**, *99*, 15222.
(18) Borry, R. W.; Kim, Y. H.; Huffsmith, A.; Reimer, J. A.; Iglesia, E. *J. Phys. Chem. B* **1999**, *103*, 5787.
(19) Kubelka, P.; Munk, F. *Z. Tech. Phys.* **1931**, *12*, 593.
(20) Barton, D. Ph.D. Dissertation, University of California, Berkeley, 1998.
(21) Ressler, T. *WinXAS97 (version 1.2)* **1998**,
(22) Li, W.; Meitzner, G. D.; Borry, R. W.; Kim, Y. H.; Iglesia, E. *Stud. Surf. Sci. Catal.* **2000**, *130*, 3621.
(23) Campbell, S. M.; Bibby, D. M.; Coddington, J. M.; Howe, R. F.; Meinhold, R. H. *J. Catal.* **1996**, *161*, 338.
(24) Pu, S. B.; Inui, T. *Zeolites* **1997**, *19*, 452.
(25) Moen, A.; Nicholson, D. G.; Ronning, M.; Lamble, G. M.; Lee, J. F.; Emerich, H. *J. Chem. Soc., Faraday Trans.* **1997**, *93*, 4071.
(26) Jiang, T.; Ellis, D. E. *J. Mater. Res.* **1996**, *11*, 2242.
(27) Bearden, J. A.; Burr, A. F. *Rev. Mod. Phys.* **1967**, *29*, 125.
(28) Biscardi, J. A.; Iglesia, E. *Phys. Chem. Chem. Phys.* **1999**, *1*, 5753.
(29) Feng, X.; Hall, W. K. *Catal. Lett.* **1997**, *46*, 11.
(30) Rice, M. J.; Bell, A. T.; Chakraborty, A. *J. Catal.* **1999**, *186*, 222.
(31) Dedecek, J.; Kaucky, D.; Wichterlova, B. *Microporous Mesoporous Mater.* **2000**, *35−36*, 483.